Investigation of two-layered turbid media with time-resolved reflectance

Alwin Kienle, Thomas Glanzmann, Georges Wagnières, and Hubert van den Bergh

Light propagation in two-layered turbid media that have an infinitely thick second layer is investigated with time-resolved reflectance. We used a solution of the diffusion equation for this geometry to show that it is possible to derive the absorption and the reduced scattering coefficients of both layers if the relative reflectance is measured in the time domain at two distances and if the thickness of the first layer is known. Solutions of the diffusion equation for semi-infinite and homogeneous turbid media are also applied to fit the reflectance from the two-layered turbid media in the time and the frequency domains. It is found that the absorption coefficient of the second layer can be more precisely derived for matched than for mismatched boundary conditions. In the frequency domain, its determination is further improved if phase and modulation data are used instead of phase and steady-state reflectance data. Measurements of the time-resolved reflectance were performed on solid two-layered tissue phantoms that confirmed the theoretical results.

OCIS codes: 120.5700, 290.1990, 290.7050, 300.6340, 330.6790.

1. Introduction

Many diagnostic and therapeutic applications of light in medicine require information about the scattering and the absorption properties of tissues. In determining these quantities, it is usually assumed that the investigated tissue is homogeneous. In many applications, however, this assumption is not valid. It is thus necessary to interpret results obtained from homogeneous models carefully or to improve the theoretical models.[1] Because of the layered structure of many parts of the body, the investigation of a layered tissue model is especially promising. Potential applications of a layered model are, for example, optical noninvasive glucose monitoring,[2] near-infrared spectroscopy to measure the hemoglobin content or the hemoglobin saturation in the brain or in muscles of the extremities,[3–5] or noninvasive determination of photosensitizer uptake in tissue.[6] Solutions for a semi-infinite and homogeneous turbid medium can be readily found in the steady-state, frequency, and time domains[7–9] by use of the diffusion approximation to the transport equation.[10] Layered turbid media have been investigated with different mathematical approaches. Several researchers have derived solutions of the diffusion equation for this geometry.[11–13] A random-walk model for the calculation of the photon migration in layered media has also been developed.[14,15] Monte Carlo simulations were applied to solve the more exact transport equation for layered media,[16,17] but determining the optical coefficients with this approach is time consuming if used in a nonlinear regression algorithm.[18]

We recently solved the diffusion equation by using the Fourier-transform approach for a two-layered turbid medium that has a semi-infinite second layer.[19] Unlike Dayan *et al.*,[13] who introduced approximations to obtain relatively simple expressions for the reflectance, we avoided any approximation by calculating the reflectance by using numerical integration. Moreover, the zero boundary condition was replaced by the more accurate extrapolated boundary condition. It was found that these results are close to those obtained from Monte Carlo simulations in the steady-state, frequency, and time domains. We also showed that it is possible to derive the absorption and the reduced scattering coefficients of both layers from steady-state-domain and frequency-domain reflectance if the thickness of the first layer is known. In the frequency domain, for example, it was found that performing relative measurements of the phase and the steady-state reflectance at three distances

The authors are with the Institute of Environmental Engineering, Swiss Federal Institute of Technology, CH-1015 Lausanne, Switzerland. A. Kienle is also with the Department of Biophysics, University of Ulm, Albert-Einstein Allee 11, D-89081 Ulm, Germany.

Received 1 May 1998; revised manuscript received 22 June 1998.
0003-6935/98/286852-11$15.00/0

from the illumination point was sufficient to obtain useful estimates of the optical properties.

In this study we investigate the possibility of deriving the optical properties of the two layers from reflectance measurements in the time domain by fitting the solutions of the two-layered diffusion equation to results obtained from this solution or from two-layered Monte Carlo simulations and to experimental data. Solutions of the diffusion equation for a semi-infinite and homogeneous medium in the time and the frequency domains were also used to fit the theoretical and the experimental two-layered reflectance data in order to investigate the conditions under which these solutions can be applied to obtain the optical coefficients of the second layer. Time-domain measurements were performed on two-layered solid tissue phantoms, with a mode-locked Nd:YLF laser as source and a streak camera as detector. We concentrated on determining the absorption coefficient of the second layer, because this quantity is especially relevant in several applications such as the determination of the hemodynamics in the brain or in muscles. In order to be able to compare the theoretical and the experimental results, we chose the optical properties of the two-layered turbid media in the theoretical investigations in accordance with those determined from the measurements on the tissue phantoms.

2. Theory

A. Diffusion Equation

In this section we present solutions of the diffusion equation for two-layered (Subsection 2.A.1) and for homogeneous, semi-infinite turbid media (Subsection 2.A.2) in the frequency and the time domains that are used in Sections 4 and 5 for the determination of the optical properties of two-layered turbid media. The origin of the coordinate system is the point where the beam enters the turbid medium. The z coordinate has the same direction as the incident beam. The x and the y coordinates lie on the surface of the turbid sample and $\rho = (x^2 + y^2)^{1/2}$. It is assumed that an infinitely thin beam is incident upon the turbid medium and that the beam is scattered isotropically at a depth of $z = z_0 = 1/(\mu_s' + \mu_a)$, where μ_s' and μ_a are the reduced scattering and the absorption coefficients, respectively, of the turbid medium (first layer of the two-layered medium). For all solutions the extrapolated boundary condition is used.[8]

1. Two-Layered Media

Recently we solved the diffusion equation for two-layered turbid media that have a first-layer thickness l and an infinitely thick second layer by using the Fourier-transform approach.[19] In order to obtain the time-domain reflectance, we first derived the solutions in the frequency domain. It was assumed that the refractive indices n of the first and the second layer were the same ($n_1 = n_2$) and that the source was sinusoidally modulated at frequency $f = \omega/(2\pi)$. For the fluence rate in layer i, $\Phi_i(\rho, z, \omega)$ we obtained[19]

$$\Phi_i(\rho, z, \omega) = \frac{\exp(j\omega t)}{2\pi} \int_0^\infty \phi_i(z, \omega, s) s J_0(s\rho) \mathrm{d}s, \quad (1)$$

where J_0 is the zeroth-order Bessel function and $\phi_1(z, \omega, s)$ is given by

$$\phi_1(z, \omega, s) = \frac{\sinh[\alpha_1(z_b + z_0)]}{D_1\alpha_1} \frac{D_1\alpha_1 \cosh[\alpha_1(l - z)] + D_2\alpha_2 \sinh[\alpha_1(l - z)]}{D_1\alpha_1 \cosh[\alpha_1(l + z_b)] + D_2\alpha_2 \sinh[\alpha_1(l + z_b)]} - \frac{\sinh[\alpha_1(z_0 - z)]}{D_1\alpha_1}, \quad 0 \le z < z_0; \quad (2)$$

$$\phi_1(z, \omega, s) = \frac{\sinh[\alpha_1(z_b + z_0)]}{D_1\alpha_1} \frac{D_1\alpha_1 \cosh[\alpha_1(l - z)] + D_2\alpha_2 \sinh[\alpha_1(l - z)]}{D_1\alpha_1 \cosh[\alpha_1(l + z_b)] + D_2\alpha_2 \sinh[\alpha_1(l + z_b)]}, \quad z_0 < z < l, \quad (3)$$

where we assumed that $l > z_0$, and for $\phi_2(z)$ we got

$$\phi_2(z) = \frac{\sinh[\alpha_1(z_b + z_0)] \exp[\alpha_2(l - z)]}{D_1\alpha_1 \cosh[\alpha_1(l + z_b)] + D_2\alpha_2 \sinh[\alpha_1(l + z_b)]}. \quad (4)$$

$D_i = 1/3(\mu_{ai} + \mu_{si}')$ is the diffusion coefficient; (Recently it was found[20–22] that it is more exact to use $D_i = 1/3\mu_{si}'$. However, this is not relevant in this study because $\mu_{si}' \gg \mu_{ai}$.); μ_{si}' and μ_{ai} are the reduced scattering and the absorption coefficients of layer i, respectively; and $\alpha_i^2 = (D_i s^2 + \mu_{ai} + j\omega/c)/D_i$. The velocity of light in the medium is c and $j = \sqrt{-1}$. The extrapolated boundary is located at $z = -z_b$, where

$$z_b = \frac{1 + R_{\mathrm{eff}}}{1 - R_{\mathrm{eff}}} 2D_1. \quad (5)$$

R_{eff} represents the fraction of photons that are internally diffusely reflected at the boundary. R_{eff} equals 0.493 for a refractive index of $n_o = 1$ outside and of $n_i = 1.4$ inside the turbid medium.[8] According to the experimental situation, the matched boundary condition ($n_o = n_i$) is mainly used in this paper, where we have $R_{\mathrm{eff}} = 0$.

The integration in Eq. (1) is performed numerically by application of Gauss's formula. The frequency-

domain reflectance $R(\rho, \omega)$ is calculated as the integral of the radiance over the backward hemisphere[8]:

$$R(\rho, \omega) = \int_{2\pi} d\Omega[1 - R_{\text{fres}}(\theta')] \frac{1}{4\pi} \left[\Phi_1(\rho, z = 0, \omega) + 3D_1 \frac{\partial}{\partial z} \Phi_1(\rho, z, \omega)|_{z=0} \cos\theta' \right] \cos\theta', \quad (6)$$

where $R_{\text{fres}}(\theta')$ is the Fresnel reflection coefficient for a photon with an incidence angle θ' relative to the normal to the boundary. For $n_i = 1.4$ and $n_o = 1$, Eq. (6) gives[9]

$$R(\rho, \omega) = 0.118\Phi_1(\rho, z = 0, \omega) + 0.306D_1 \frac{\partial}{\partial z} \Phi_1(\rho, z,\omega)|_{z=0}, \quad (7)$$

and for the matched boundary condition we get

$$R(\rho,\omega) = \frac{1}{4} \Phi_1(\rho, z = 0, \omega) + \frac{1}{2} D_1 \frac{\partial}{\partial z} \Phi_1(\rho, z, \omega)|_{z=0}. \quad (8)$$

The phase angle θ between the source and the detected signal and the modulation M is given by

$$\theta = \tan^{-1} \frac{\text{Im}[R(\rho, \omega)]}{\text{Re}[R(\rho, \omega)]}, \quad (9)$$

$$M = \left\{ \frac{[\text{Im } R(\rho, \omega)]^2 + [\text{Re } R(\rho, \omega)]^2}{[R(\rho, \omega = 0)]^2} \right\}^{1/2}. \quad (10)$$

The steady-state reflectance $R(\rho)$ is calculated with Eq. (8) [Eq. (7)]:

$$R(\rho) = R(\rho, \omega = 0). \quad (11)$$

The time-domain reflectance $R(\rho, t)$ is obtained by calculation of the real and the imaginary parts of the reflectance in the frequency domain $R(\rho, \omega)$ at many frequencies and by fast Fourier transforms of these data.[19]

2. *Semi-Infinite and Homogeneous Media*

The fluence rate for semi-infinite and homogeneous turbid media in the frequency domain is[8]

$$\Phi(\rho, z, \omega) = \frac{\exp(j\omega t)}{4\pi D} \left(\frac{\exp\{-k[(z - z_0)^2 + \rho^2]^{1/2}\}}{[(z - z_0)^2 + \rho^2]^{1/2}} - \frac{\exp\{-k[(z + z_0 + 2z_b)^2 + \rho^2]^{1/2}\}}{[(z + z_0 + 2z_b)^2 + \rho^2]^{1/2}} \right), \quad (12)$$

where $k = [(\mu_a c + i\omega)/Dc]^{1/2}$. We calculate the reflectance by inserting Eq. (12) into Eq. (7) or Eq. (8) and the phase, modulation, and steady-state reflectance are obtained with Eqs. (9), (10), and (11), respectively.

The time-domain fluence rate is given by[7]

$$\Phi(\rho, z, t) = \frac{c}{(4\pi Dct)^{3/2}} \exp(-\mu_a ct) \times \left\{ \exp\left[-\frac{(z - z_0)^2 + \rho^2}{4Dct} \right] - \exp\left[-\frac{(z + z_0 + 2z_b)^2 + \rho^2}{4Dct} \right] \right\}. \quad (13)$$

We calculate the time-domain reflectance by inserting Eq. (13) into Eq. (7) or Eq. (8) (where ω has to be replaced by t).

B. Monte Carlo Simulations

In Section 4 the solutions of the diffusion equation are fitted to reflectance data obtained from Monte Carlo simulations. The Monte Carlo method of photon transport in turbid media has been thoroughly described in literature.[23] The essential features of our code are listed below. For illumination of the two-layered tissue, a pencil beam was used. The Henyey–Greenstein[24] phase function, which has an anisotropy factor g of 0.8, was used for calculation of the scattering angle. A refractive index of 1.4 was applied to both layers and to the surrounding medium (matched boundary condition). The Monte Carlo simulations were performed in the time domain. The fast Fourier transform was used to obtain the steady-state reflectance, the phase, and the modulation. $R(\rho, t)$, for different absorption coefficients in the second layer, was obtained from one simulation by the scoring of the lengths of the photon paths in the second layer and application of Beer's law.[25,26]

C. Nonlinear Regression

A combination of the gradient search method and the method of linearizing the fitting function[27] was implemented for the nonlinear regression. The logarithm of the reflectance was fitted for the investigations in the time domain. The time range for the nonlinear regression of $R(\rho, t)$ was chosen as follows: the start time was variable and the end time was $R_{\text{max}}/1000$, where R_{max} is the maximum value of the reflectance curve. The end time was reduced if the Monte Carlo simulations or the experiments showed large statistical noise in this time range. Relative phase values (the phase difference determined at adjacent distances) and relative steady-state reflectance or modulation values (the ratio determined at adjacent distances) were used for the investigations in the frequency domain. For all data points, equal weights were applied in the fitting procedure.

3. Materials and Methods

In Section 5 the solutions of the diffusion equation are used to fit experimental results obtained from measurements on solid phantoms in the time domain. 70-ps-pulses at a wavelength of $\lambda = 528$ nm, generated from a mode-locked and frequency-doubled Nd:YLF laser (Antares 76-YLF, Coherent, Palo Alto,

Calif.), were incident upon the surface of the phantoms by an optical fiber with a 600-μm core diameter. The same type of fiber collected the scattered light at distances between $\rho = 14$ and 25 mm from the source. A black cylindrical probe was manufactured and placed onto the phantom. Holes were drilled into the probe to hold the detection and the source fibers in contact with the surface of the phantom and at a precise distance from each other. The black probe also served as a photon sink. The detector was a streak camera (C4334, Hamamatsu, Hamamatsu City, Japan) with a maximum temporal resolution of 15 ps, coupled to a spectrograph. The detector part was described in detail in Ref. 28. It can be used in the analog mode and in the photon-counting mode. The analog mode of the streak camera was applied for the experiments presented here because it is faster, and, furthermore, both modes were found to be equally accurate in determining the optical coefficients from experiments.

To determine the optical properties in the time domain with nonlinear regressions, we considered the duration of the incident laser pulse by convolving the measured laser pulse with the theoretical solutions for the time-resolved reflectance (which were derived for a delta pulse). For this purpose, the laser pulse was measured with the streak camera before each experiment on the phantoms. We did this by replacing the phantom with a black sheet of aluminium that was positioned several centimeters below the fibers and by measuring the reflected pulse. We were able to determine the time when the pulse left the source fiber by knowledge of the distance between the fibers and the sheet. The zero time of the reflectance measurements on the phantoms could thus be obtained from these measurements. This procedure requires a stable laser source with a small jitter.

The time-resolved reflectance measurements were made on two-layered solid tissue phantoms.[19,29] The basic medium was two-component transparent silicone, which cures at room temperature. Before the base and the catalyst were mixed, the scattering and the absorbing particles were added. Polystyrene spheres with a 2.5-μm diameter and graphite powder were used as scattering and absorbing material. Two two-layered phantoms were manufactured, one consisting of a 2-mm-thick first layer (phantom 1) and the other of a 6-mm-thick first layer (phantom 2). The first layer of phantom 1 (phantom 2) was made from the same material as that of the second layer of phantom 2 (phantom 1). Thus measurements on the side of the second layer of the two phantoms allowed us to derive the optical properties of the layers separately. The solution of the diffusion equation for a semi-infinite medium could be applied in these measurements, because the first layer does not influence the light propagation. The lateral dimensions of the smaller phantom were 9 cm × 9 cm and the height was 6 cm, which eliminated any influence from the lateral boundaries. Below we considered mainly the phantom with a thickness of 6 mm because it is more difficult to obtain the optical properties of the second layer when the first-layer thickness is great.

The black probe that served as a holding device for the fibers was made of polyoxymethylene, which has a refractive index of $n_o = 1.48$. The refractive index of the tissue phantoms is close to $n_i = 1.4$.[29,30] The fraction of photons that are internally reflected is low for this boundary condition ($R_{\text{eff}} = 0.010$) because of the absence of total internal reflection. For the measurements, the matched boundary condition is assumed (the polyoxymethylene probe stuck to the phantoms so that no air layer was formed between them), because it was found that this approximation causes errors of less than 1% in determining the optical properties.

4. Determination of the Optical Properties from Nonlinear Regression to Solutions of the Diffusion Equation or to Monte Carlo Simulations

In this section we present the optical properties obtained from nonlinear regressions of the solution of the diffusion equation for a two-layered turbid medium and of the semi-infinite and homogeneous solutions to results calculated with the two-layered diffusion equation or with two-layered Monte Carlo simulations. Unless otherwise stated, the matched boundary condition was used. For the investigated two-layered turbid media, the reduced scattering coefficients of the first and the second layers and the absorption coefficient of the first layer were chosen according to those of phantom 2. The absorption coefficient of the second layer was varied to simulate measurements of the hemodynamics, for example, in the brain or in muscles.

To demonstrate the influence of the two layers on the time-resolved reflectance, Fig. 1 shows $R(\rho, t)$ from a two-layered medium [$R_t(\rho, t)$, solid curve] and the reflectance from two semi-infinite and homogeneous turbid media that have the same optical properties as the first layer [$R_1(\rho, t)$, short-dashed curve] and the second layer [$R_2(\rho, t)$, long-dashed curve) of the two-layered turbid medium. These curves were calculated with the corresponding solutions of the diffusion equation presented in Subsection 2.A. (For the optical coefficients and the thickness of the first layer we used the values of phantom 2.) For comparison the Monte Carlo simulation for the two-layered medium (open circles) is also shown. It can be seen that $R_t(\rho, t)$ is almost identical to $R_1(\rho, t)$ until $t \approx 250$ ps, indicating that the photons propagated predominantly in the first layer. For longer times, $R_t(\rho, t)$ is located between $R_1(\rho, t)$ and $R_2(\rho, t)$. Finally, $R_t(\rho, t)$ approaches a similar slope as $R_2(\rho, t)$. This means that these late-arriving photons propagated mostly in the second layer. Therefore it is possible, in several cases, to determine the absorption coefficient of the second layer by using a semi-infinite and homogeneous model.[16] The reflectance calculated with the Monte Carlo method is close to $R_t(\rho, t)$ for times greater than $t \approx 200$ ps. For earlier times the differences are caused by the failure of the diffusion approximation.

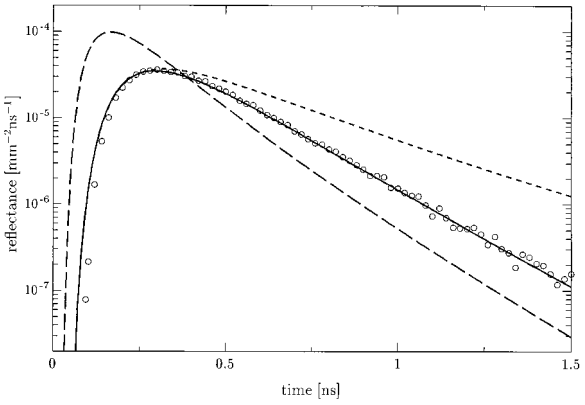

Fig. 1. Time-resolved reflectance from a two-layered turbid medium calculated with the diffusion equation (solid curve) and with Monte Carlo simulations (open circles) are shown. The thickness of the first layer is $l = 6$ mm. The optical parameters are $\mu'_{s1} = 1.28$ mm^{-1}, $\mu_{a1} = 0.0074$ mm^{-1}, $\mu'_{s2} = 0.67$ mm^{-1}, and $\mu_{a2} = 0.019$ mm^{-1}. Also shown are $R(\rho, t)$ for semi-infinite and homogeneous media calculated with $\mu'_s = 1.28$ mm^{-1}, $\mu_a = 0.0074$ mm^{-1} (short-dashed curve) and $\mu'_s = 0.67$ mm^{-1}, $\mu_a = 0.019$ mm^{-1} (long-dashed curve). The matched boundary condition is assumed ($n_i = n_o = 1.4$), and the distance ρ equals 14.5 mm.

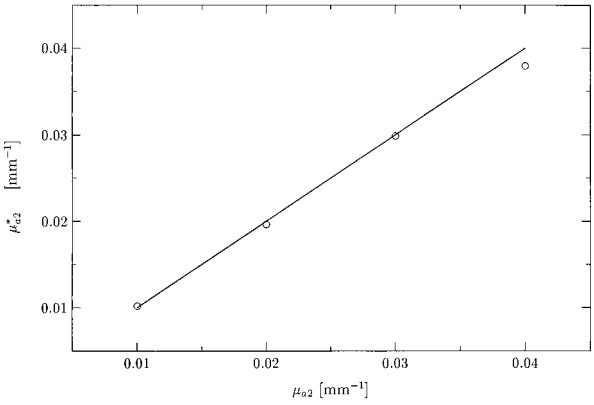

Fig. 2. Estimated absorption coefficients (μ^*_{a2}) (open circles) of the second layer determined by nonlinear regressions of time-resolved reflectance by use of the two-layered solution of the diffusion equation to Monte Carlo data are shown versus the true absorption coefficient of the second layer used in the Monte Carlo simulations (μ_{a2}). The optical parameters of the Monte Carlo simulations are $\mu'_{s1} = 1.28$ mm^{-1}, $\mu_{a1} = 0.0074$ mm^{-1}, and $\mu'_{s2} = 0.67$ mm^{-1}, and μ_{a2} is varied between $\mu_{a2} = 0.01$ mm^{-1} and $\mu_{a2} = 0.04$ mm^{-1}. The thickness of the first layer is $l = 6$ mm. The line indicates μ_{a2}. Relative time-resolved reflectance data at distances $\rho = 14.5$ and 19.5 mm were used in the nonlinear regression.

A. Nonlinear Regressions by Use of Solutions of the Two-Layered Diffusion Equation

In this subsection we investigate what information can be obtained from measurements of the reflectance from a two-layered medium in the time domain if no approximations in the theoretical model are made. For this purpose, we used the solution of the two-layered diffusion equation in the time domain presented in Subsection 2.A.1 for nonlinear regression to data that were calculated with the same solution. It was assumed that the time-resolved reflectance was measured at two distances from the source.

We first examined the possibility of determining the absorption and the reduced scattering coefficients of the two layers and the thickness of the first layer. For this purpose absolute time-resolved reflectance data at two distances were used. It was found that these five parameters can, in principle, be determined, but the convergence of the nonlinear regression is slow and, in addition, the start parameters must be close to the real ones. We note that similar results were obtained from investigations in the steady-state and the frequency domains.[19,31] Thus we assume below that the thickness of the first layer is known.

Next we investigated the possibility of deriving the optical coefficients with relative time-resolved reflectance measurements at two distances. This means that six parameters, the absorption and the reduced scattering coefficients of the two layers and a multiplicative constant for the time-resolved reflectance at each distance, were fitted. It was found by nonlinear regressions to data calculated with the diffusion equation that these optical parameters can be correctly obtained and that the convergence is faster than in the case in which the first layer thickness is also fitted.

For examining more realistic situations, the time-domain solution of the two-layered diffusion equation was used to fit reflectance data at two distances obtained from the more exact two-layered Monte Carlo simulations. Thus the influence of the diffusion approximation and that of statistical noise arising from the Monte Carlo simulations could be investigated. The number of photons used in the Monte Carlo simulations was chosen so that the statistical noise of the time-domain reflectance was comparable with the experimental noise of the measurements with the streak camera. Reflectance data that begin at $R(\rho, t) = 9/10R_{\max}$ (before the maximum reflectance value $R_{\max}$) were used for the nonlinear regressions. Measurements of the relative time-resolved reflectance were assumed, i.e., six parameters were fitted. Figure 2 shows the absorption coefficients of the second layer (μ^*_{a2}) obtained from the nonlinear regressions. Time-resolved reflectance curves at $\rho = 14.5$ and 19.5 mm were used. The correct values of μ_{a2} are also depicted in the figure. Figure 2 shows that it is possible to determine the absorption coefficients of the second layer with errors of less than a few percent. The differences between the derived and the correct values are caused mainly by the uncertainties in the Monte Carlo simulations. The other optical coefficients (not shown) have greater errors, especially the absorption coefficient of the first layer, which shows differences of up to 20%. This is caused by the relatively small contribution of μ_{a1} to the shape of the time-domain reflectance curve.

B. Nonlinear Regressions by Use of Solutions of the Homogeneous and Semi-Infinite Diffusion Equation

In this subsection the homogeneous and semi-infinite solutions presented in Subsection 2.A.2 are used to fit two-layered reflectance data calculated with the so-

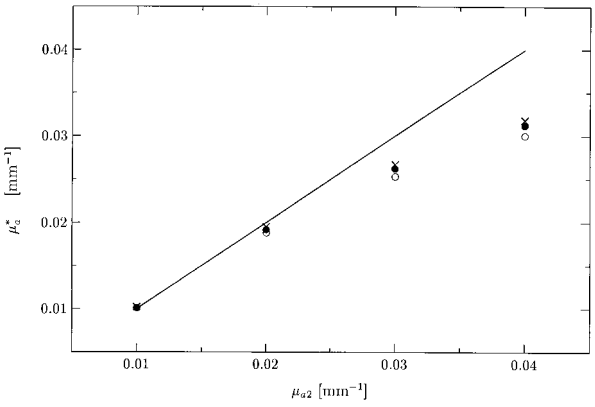

Fig. 3. Estimated absorption coefficients (μ_a^*) determined by nonlinear regressions of time-resolved reflectance with the homogeneous solution of the diffusion equation to two-layered data are shown versus the true absorption coefficient of the second layer (μ_{a2}). The optical parameters of the two-layered medium are $\mu_{s1}' = 1.28\ \text{mm}^{-1}$, $\mu_{a1} = 0.0074\ \text{mm}^{-1}$, and $\mu_{s2}' = 0.67\ \text{mm}^{-1}$, and μ_{a2} is varied between $\mu_{a2} = 0.01\ \text{mm}^{-1}$ and $\mu_{a2} = 0.04\ \text{mm}^{-1}$. The thickness of the first layer is $l = 6$ mm. The line indicates μ_{a2}. Results for time-resolved reflectance data at distances $\rho = 14.5$ (open circles), $\rho = 19.5$ (filled circles), and $\rho = 24.5$ mm (crosses) are shown.

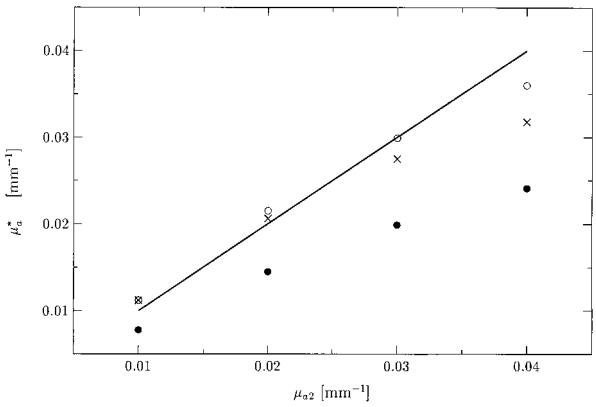

Fig. 4. Estimated absorption coefficients (μ_a^*) determined by nonlinear regressions of the homogeneous solution of the diffusion equation in the frequency domain to two-layered data are shown versus the true absorption coefficient of the second layer (μ_{a2}). The optical parameters of the two-layered medium are $\mu_{s1}' = 1.28\ \text{mm}^{-1}$, $\mu_{a1} = 0.0074\ \text{mm}^{-1}$, and $\mu_{s2}' = 0.67\ \text{mm}^{-1}$, and μ_{a2} is varied between $\mu_{a2} = 0.01\ \text{mm}^{-1}$ and $\mu_{a2} = 0.04\ \text{mm}^{-1}$. The thickness of the first layer is $l = 6$ mm. The line indicates μ_{a2}. Results from nonlinear regression by phase and steady-state reflectance (filled circles) and phase and modulation data (open circles) are depicted. The matched boundary condition is used ($n_o = n_i = 1.4$). Also shown are μ_a^* determined from the same two-layered media by use of modulation and phase data, but the mismatched boundary condition ($n_o = 1.0$, $n_i = 1.4$) is applied (crosses). Relative data between $\rho = 14.5$ and 24.5 mm are used in the nonlinear regression.

lutions of the two-layered diffusion equation (Subsection 2.A.1). Examinations in the time domain are followed by investigations in the frequency domain.

In the time domain, μ_a, μ_s', and a multiplicative constant were fitted. Figure 3 shows the absorption coefficients obtained from nonlinear regression of Eq. (8) [Eq. (13)] at one distance to two-layered reflectance data. Results from nonlinear regressions at three distances, $\rho = 14.5$, 19.5, and 24.5 mm, are shown. The absorption coefficient obtained from the semi-infinite model equals that of the second layer from the two-layered model for $\mu_{a2} = 0.01\ \text{mm}^{-1}$. For larger μ_{a2}, the derived absorption coefficients are smaller than μ_{a2} because the number of remitted photons that have been in the second layer decreases when the absorption of the second layer is increased. This behavior has already been reported by Hielscher *et al.*[16] Figure 3 shows that μ_a^* is closer to μ_{a2} if the distance between the source and the detector is increased, because of the increase in the penetration depth of the remitted photons.

In the frequency domain, several methods exist to determine the optical coefficients of turbid media. For example, it is possible to use any combination of at least two quantities of the phase, the modulation, and the steady-state reflectance at one modulation frequency. In addition, the phase or the modulation at different modulation frequencies can also be used.[32] In general, all methods result in different optical properties when applied to two-layered media.

In order to examine some of these methods quantitatively, we fitted the solutions of the homogeneous and semi-infinite diffusion equation in the frequency domain to reflectance data calculated with the two-layered diffusion equation. A modulation frequency of 195 MHz was used for these investigations. Figure 4 shows the absorption coefficients obtained for the same turbid two-layered media that were described in Fig. 3. The phase difference and the steady-state reflectance ratio (filled circles) as well as the phase difference and the modulation ratio (open circles) between $\rho = 14.5$ mm and $\rho = 24.5$ mm were used in the nonlinear regression. Relative values of the phase, modulation, and steady-state reflectance at two distances were applied because the determination of the optical coefficients from absolute quantities at one distance is not always unique.[33] Figure 4 shows that the absorption coefficients obtained from the two methods are considerably different. Whereas μ_a^* determined from the phase difference and the steady-state reflectance ratio is much lower than μ_{a2}, the absorption coefficients derived from the phase difference and the modulation ratio have errors of less than 15%. Comparing Fig. 3 with Fig. 4, we can see that the absorption coefficients obtained from the time-domain investigations are between those that have been obtained in the frequency domain. Similar investigations of two-layered media that have other optical properties and thicknesses of the first layer have been performed. In general, the same behavior as described above was observed for all investigated media.

Figure 4 also shows μ_a^* derived from the same turbid media by use of modulation and phase data, but now the mismatched boundary condition is used ($n_o = 1.0$, $n_i = 1.4$) (crosses). When the results are compared with the corresponding matched data

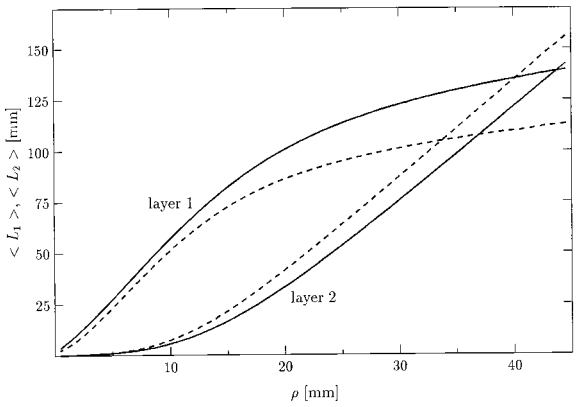

Fig. 5. Mean optical path lengths in the first and the second layers of a two-layered medium versus distance ρ by use of matched (dashed curves) and mismatched (solid curves) boundary conditions. The optical parameters of the two-layered medium are $\mu'_{s1} = 1.28\ \text{mm}^{-1}$, $\mu_{a1} = 0.0074\ \text{mm}^{-1}$, $\mu'_{s2} = 0.67\ \text{mm}^{-1}$, and $\mu_{a2} = 0.019\ \text{mm}^{-1}$. The thickness of the first layer is $l = 6$ mm.

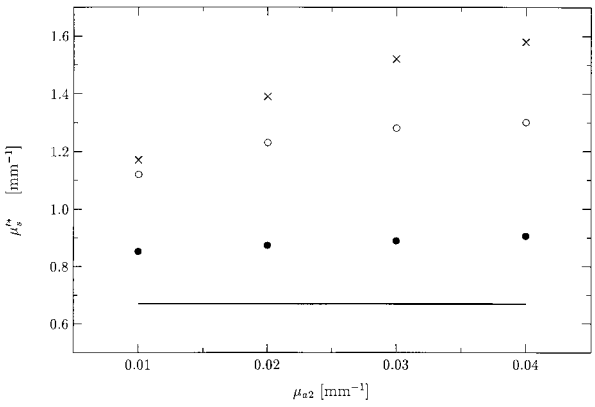

Fig. 6. Estimated reduced scattering coefficients (μ_s^*) determined by nonlinear regressions of the homogeneous solution of the diffusion equation in the frequency domain to two-layered data are shown versus the true absorption coefficient of the second layer (μ_{a2}). The optical parameters of the two-layered medium are $\mu'_{s1} = 1.28\ \text{mm}^{-1}$, $\mu_{a1} = 0.0074\ \text{mm}^{-1}$, and $\mu'_{s2} = 0.67\ \text{mm}^{-1}$, and μ_{a2} is varied between $\mu_{a2} = 0.01\ \text{mm}^{-1}$ and $\mu_{a2} = 0.04\ \text{mm}^{-1}$. The thickness of the first layer is $l = 6$ mm. The line indicates μ'_{s2}. Results from nonlinear regression by phase and steady-state reflectance (solid circles) and phase and modulation data (open circles) are shown. Relative data between ρ = 14.5 and 24.5 mm are used. Also shown is μ_s^* obtained from nonlinear regressions in the time domain at ρ = 19.5 mm. The matched boundary condition is used.

(open circles), it can be stated that μ_a^* is closer to μ_{a2} for the matched than for the mismatched boundary condition if μ_{a2} is large. This effect was also observed for all investigated turbid media. For this behavior to be explained, it has to be taken into consideration that the penetration depth of the photons is greater for the matched than for the mismatched boundary condition. For demonstrating this effect, the mean optical path length in layer $i[\langle L_i(\rho)\rangle]$ was calculated versus ρ for a two-layered medium. $\langle L_i(\rho)\rangle$ can be obtained from the modified Beer's law[34]:

$$\langle L_i(\rho)\rangle = -\Delta[\ln R(\rho)]/\Delta\mu_{ai}, \tag{14}$$

where $R(\rho)$ is calculated with Eq. (11), with Eq. (7) for the mismatched and Eq. (8) for the matched boundary condition. The results for a two-layered medium that has the same optical properties as those of phantom 2 can be seen in Fig. 5. Matched ($n_o = n_i = 1.4$, dashed curves) and mismatched ($n_o = 1.0$, $n_i = 1.4$, solid curves) boundary conditions were applied. Figure 5 shows that, for all distances, the mean optical path length of the first layer is greater for the mismatched boundary condition than it is for the matched boundary condition, whereas it is vice versa for $\langle L_2(\rho)\rangle$. The apparent smaller penetration depth for the mismatched boundary condition is caused by the total reflection of the photons that approach the boundary from inside the turbid medium.

The reduced scattering coefficients obtained from the nonlinear regressions that are presented in Fig. 4 for the matched boundary condition are depicted in Fig. 6. It can be seen that, in contrast to the determination of the absorption coefficients, the reduced scattering coefficients, obtained from the nonlinear regression of the phase and steady-state reflectance (solid circles), are closer to the values of the second layer (μ'_{s2}) compared with the coefficients obtained from the phase and modulation data (open circles). The reduced scattering coefficients obtained from the investigation in the time domain at ρ = 19.5 mm presented in Fig. 3 are also depicted in Fig. 6. Here, the reduced scattering coefficients are even larger than μ'_{s1} except for $\mu_{a2} = 0.01\ \text{mm}^{-1}$.

It is obvious that the determination of the absorption coefficient of the second layer by use of homogeneous and semi-infinite models becomes problematic when the thickness of the first layer is increased. Figure 7 shows the absorption coefficients derived from the same turbid media as those used for Fig. 4, but the thickness of the first layer is increased to 10 mm. Phase difference and steady-state reflectance ratio (solid circles) and phase difference and modulation ratio (open circles) are used in the nonlinear regression. As expected, the obtained absorption coefficients are smaller than those presented in Fig. 4 (with the exception of $\mu_{a2} = 0.01\ \text{mm}^{-1}$), but μ_a^*, determined from phase and modulation data, are still closer to μ_{a2} than μ_a^*, determined from phase and steady-state reflectance data. Similar to those in Fig. 4, the μ_a^* determined with the matched boundary condition are closer to μ_{a2} than those obtained with the mismatched boundary condition.

5. Determination of the Optical Properties from Nonlinear Regressions to Time-Resolved Measurements on Phantoms

Time-resolved reflectance measurements were carried out on the side of the two-layered phantoms to derive their optical coefficients. Figure 8 shows time-resolved reflectance measurements on the side of phantom 1 at three distances ρ equal to 14, 18, and 20 mm (solid curves). As explained in Section 3, the semi-infinite model can be used for these measure-

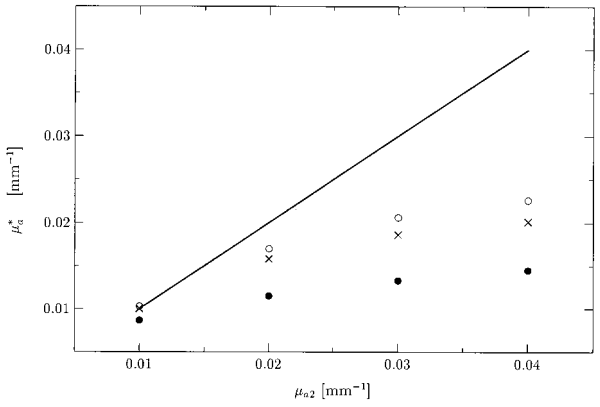

Fig. 7. Estimated absorption coefficients (μ_a^*) determined by nonlinear regressions of the homogeneous solution of the diffusion equation in the frequency domain to two-layered data are shown versus the true absorption coefficient of the second layer (μ_{a2}). The optical parameters of the two-layered medium are $\mu_{s1}' = 1.28$ mm^{-1}, $\mu_{a1} = 0.0074$ mm^{-1}, and $\mu_{s2}' = 0.67$ mm^{-1}, and μ_{a2} is varied between $\mu_{a2} = 0.01$ mm^{-1} and $\mu_{a2} = 0.04$ mm^{-1}. The thickness of the first layer is $l = 10$ mm. The line indicates μ_{a2}. Results from nonlinear regression by use of phase and steady-state reflectance (solid circles) and phase and modulation data (open circles) are depicted. The matched boundary condition is used ($n_o = n_i = 1.4$). Also shown are μ_a^* determined from the same two-layered media by use of modulation and phase data, but the mismatched boundary condition ($n_o = 1.0$, $n_i = 1.4$) is applied (crosses). Relative data between $\rho = 14.5$ and 24.5 mm are used in the nonlinear regression.

ments. Thus Eq. (8), with Eq. (13), was applied to determine the optical coefficients from $R(\rho, t)$ at one distance. The parameter σ of the Gaussian curve was determined by nonlinear regression to the measured pulse profile. Time-resolved measurements were made at several distances. For each measurement the optical coefficients were determined. In addition, for each measurement, μ_a and μ_s' were determined for different start values of the time-

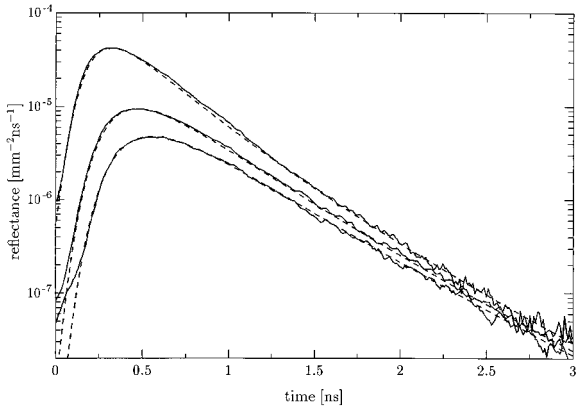

Fig. 8. Time-resolved reflectance measurements on the side of phantom 1 (semi-infinite and homogeneous geometry) at three distances $\rho = 14$, 18, and 20 mm (solid curves) are shown. The theoretical time-resolved reflectance is also depicted (dashed curves). The optical parameters used in the calculations are $\mu_s' = 1.28$ mm^{-1} and $\mu_a = 0.0074$ mm^{-1}. The theoretical curves are convolved with a Gaussian curve with $\sigma = 60$ ps.

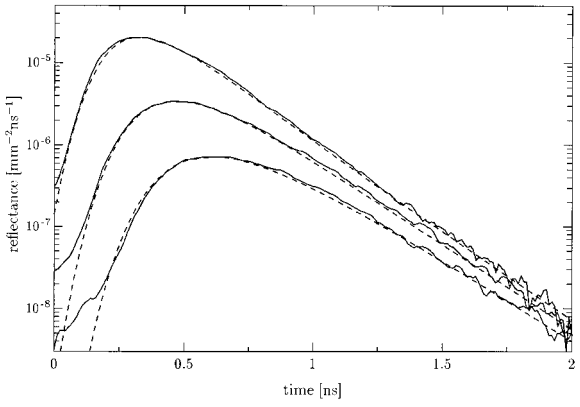

Fig. 9. Time-resolved reflectance measurements on the top of phantom 2 (two-layered geometry) at three distances $\rho = 15$, 20, and 25 mm (solid curves) are shown. The theoretical time-resolved reflectance (dashed curves) is also depicted. The optical parameters used are $\mu_{s1}' = 1.28$ mm^{-1}, $\mu_{a1} = 0.0074$ mm^{-1}, $\mu_{s2}' = 0.67$ mm^{-1}, and $\mu_{a2} = 0.019$ mm^{-1}. The thickness of the first layer is $l = 6$ mm. The theoretical curves are convolved with a Gaussian curve ($\sigma = 60$ ps).

resolved reflectance curve. The absorption and the reduced scattering coefficients and a multiplicative factor were fitted. For the second layer of phantom 1 we obtained $\mu_s' = 1.28 \pm 0.10$ mm^{-1} and $\mu_a = 0.0074 \pm 0.0005$ mm^{-1}. Figure 8 shows the theoretical time-resolved reflectance calculated with these optical parameters (dashed curves). The experimental data were normalized to the maximum value of the theoretical curves. The theoretical curves are close to the experiments, except in the earlier times, when the experiments show higher values than those of the theory. These differences are caused by the scattering of photoelectrons in the streak camera. The optical properties of the second layer of phantom 2 were determined in the same manner. We obtained $\mu_s' = 0.67 \pm 0.07$ mm^{-1} and $\mu_a = 0.019 \pm 0.001$ mm^{-1}.

Figure 9 shows measurements of the time-resolved reflectance on the top of phantom 2 (two-layered geometry) at three distances ρ equal to 15, 20, and 25 mm. For comparison, theoretical curves are also shown in Fig. 9. They were calculated with the solution of the diffusion equation for two-layered media by use of the optical coefficients that had been determined from the measurements on the side of the phantoms. The experimental curves were normalized to the maximum of the theoretical curves. The zero times of the experimental curves were obtained by measurement of the pulse before each experiment on the phantoms, as described in Section 3. To determine the optical coefficients of the two-layered media, we used the solution of the diffusion equation for two layers to perform nonlinear regressions to the experimental data shown in Fig. 9. Time-resolved measurements at two distances (15 and 20, 15 and 25, or 20 and 25 mm) were used. In addition, we varied the fitting range by changing the start times of $R(\rho, t)$ in the nonlinear regression. Six parameters,

Table 1. Optical Coefficients Derived from Measurements on the Top of Phantom 2 (Two-Layered Geometry, l = 6 mm) by Use of the Semi-Infinite Model in the Time Domain in the Nonlinear Regression and the Results from Nonlinear Regressions to Data Obtained from the Two-Layered Diffusion Equations

	Experiment		Diffusion Equation	
ρ (mm)	μ_s' (mm^{-1})	μ_a (mm^{-1})	μ_s' (mm^{-1})	μ_a (mm^{-1})
15	1.56	0.0183	1.44	0.0181
20	1.39	0.0184	1.37	0.0184
25	1.38	0.0192	1.28	0.0186

the absorption and the reduced scattering coefficients of both layers and a multiplicative constant for each time-resolved reflectance curve, were fitted. We found that μ_{s1}' and μ_{a2} could be determined within 10% of the values derived from the measurements on the semi-infinite media, whereas the errors in determining μ_{s2}' and μ_{a1} were considerably greater. In addition, the derived μ_{s2}' and μ_{a1} depended on the start parameters of the nonlinear regression. This behavior is not surprising, considering the results of the nonlinear regressions to Monte Carlo data discussed in Subsection 4.A.

We note that the optical coefficients of phantom 1 were derived in the same way as those of phantom 2. From the nonlinear regressions to the measurements on the two-layer medium (with the two-layer model) μ_{s1}', μ_{s2}', and μ_{a2} could be determined within 10% of the values obtained from the measurements on the semi-infinite media. However, no reasonable value was derived for the absorption coefficient of the first layer, as this parameter has a relatively small influence on the time-resolved reflectance curve.

As in Subsection 4.B, the semi-infinite equations in the time and the frequency domains were also used to derive the optical properties from the measurements on phantom 2. Table 1 summarizes the optical coefficients obtained from the nonlinear regression of Eq. (8) with Eq. (13) to the experiments performed at ρ equal to 15, 20, and 25 mm. The results obtained from fitting these equations to reflectance data, calculated with the two-layered solution of the diffusion equation, are shown for comparison. The optical coefficients, derived from the experimental data, are close to those obtained from the theoretical data.

Finally, we compared the optical coefficients derived with the semi-infinite and the homogeneous solutions in the frequency domain. The time-domain reflectance measurements at ρ equal to 15, 20, and 25 mm were Fourier transformed, and phase, modulation, and steady-state reflectance data were obtained. As in Subsection 4.B we fitted the phase difference and the modulation ratio and the phase difference and the steady-state reflectance ratio between two distances (15/20 mm, 15/25 mm, or 20/25 mm) at f = 195 MHz. We note that it is not necessary to deconvolve the time-domain reflectance measurements with the laser pulse because the phase difference between different distances is calculated and therefore the effect of the deconvolution cancels out. The mean optical absorption coefficient, derived from nonlinear regressions to phase and modulation data (phase and steady-state reflectance) at the different combinations of distances, was found to be $\mu_a = 0.022 \pm 0.002\ mm^{-1}$ ($\mu_a = 0.014 \pm 0.002\ mm^{-1}$). The corresponding value from nonlinear regressions to frequency-domain reflectance calculated with the two-layered diffusion equation is $\mu_a = 0.021 \pm 0.001\ mm^{-1}$ ($\mu_a = 0.014 \pm 0.001\ mm^{-1}$) and thus within the standard deviation of the experimental data.

6. Discussion

The solution of the diffusion equation for a two-layered turbid medium has been used to investigate the determination of the optical properties from time-resolved reflectance at two distances from the source. It was found that the absorption and the reduced scattering coefficients of both layers and the thickness of the first layer can, in principle, be derived if absolute measurements of $R(\rho)$ are made at two distances from the source. However, similar to the results obtained in the steady-state and the frequency domains,[19] the convergence of the nonlinear regressions was slow and the start parameters of the fit had to be close to the true optical coefficients.

Thus we concentrated on the determination of the absorption and the reduced scattering coefficients, knowing the thickness of the first layer. We showed that, by fitting the solution of the diffusion equation for two-layered media to Monte Carlo simulations, it is possible to obtain the four optical parameters from relative (a multiplicative constant was fitted for each distance) time-resolved reflectance measurements at two distances. The optical coefficients were determined with errors of less than a few percent for optical properties that are typical of biological tissue.

Measurements of the time-resolved reflectance were performed on turbid two-layered phantoms. First we derived the optical properties of the phantom layers by measuring the relative reflectance from a semi-infinite geometry at one distance. The reduced scattering and absorption coefficients could be found with differences of ≈10% and less than 10%, respectively, as judged through the comparison of experiments at different distances. For the two-layered geometry we could show that the measured $R(\rho, t)$ was close to the theoretical reflectance, calculated with the optical properties determined from the measurements in the semi-infinite geometry. We fitted the solution of the diffusion equation for two-layered turbid media to the experimental reflectance measured at two distances and determined μ_{a2} and μ_{s1}' with errors of less than 10%, whereas the errors in deriving the other optical properties were greater. This is caused by systematic errors in the measurements that influence mainly the optical properties, which do not strongly determine the shape of the reflectance curve. However, μ_{a2}, which is important for many applications, could be accurately derived.

We can improve the results by measuring $R(\rho, t)$ at more distances[35] and by measuring the absolute $R(\rho, t)$. Absolute reflectance can, for example, be obtained from additional measurements of $R(\rho, t)$ from phantoms with known optical coefficients. These improvements might be necessary for the investigation of biological tissue, because it does not consist of homogeneous layers with flat borders.

In the literature, mostly semi-infinite and homogeneous models are used to derive the optical properties of tissue. We investigated the obtained optical coefficients when semi-infinite and homogeneous models in the frequency and the time domains are applied to reflectance from two-layered turbid media. We found, experimentally and theoretically, that the different methods for the determination of μ_a and μ_s' from semi-infinite models in the time and frequency domains show considerable differences in these quantities. For large μ_{a2} and l it is possible to derive the absorption coefficient of the second layer more precisely from phase and modulation than from phase and steady-state reflectance, whereas the absorption coefficients obtained from the time-domain reflectance are between these values. In general, this behavior can easily be used to check as to whether the investigated turbid medium is homogeneous; this being the case, the derived optical properties would be the same.

The determination of the optical coefficients of two-layered turbid media with semi-infinite models was also investigated for different refractive indices of the turbid medium and the surrounding medium. For large μ_{a2} and l it was shown that the absorption coefficient of the second layer can be obtained more precisely for the matched than for the mismatched boundary condition. This can be explained by the greater penetration depth of the light remitted at a certain distance from the source, if the matched boundary condition is applied. Another possibility of increasing the penetration depth of photons is to measure at greater distances from the source, but the influence on the determination of μ_{a2} is relatively small. For example, the improvement in determining μ_{a2} by increasing ρ from 15 to 35 mm (data not shown) is smaller than that obtained by changing n_o from 1.0 to 1.4 ($n_i = 1.4$) for phantom 2. Whereas the refractive index of the surrounding medium can easily be changed, the increase of the distance between the source and the detection results in a decrease of the measured signal and of the spatial resolution.

The time-resolved measurements were performed with a mode-locked Nd:YLF laser. Before each experiment on the phantoms, the pulse of the laser was measured in order to derive the pulse duration and the calibration of the time when the photons are incident upon the phantoms. This procedure is demanding on the stability of the laser pulses. We recommend measuring the pulse and the reflectance from the phantom simultaneously, in the same experiment, in order to be less dependent on the stability of the laser output.

The optical properties of the phantoms used in this study were recently measured with absolute steady-state spatially resolved reflectance.[19] The optical coefficients for phantom 2 measured at $\lambda = 543$ nm were $\mu_{s1}' = 1.05\ \text{mm}^{-1}$, $\mu_{a1} = 0.009\ \text{mm}^{-1}$, $\mu_{s2}' = 0.52\ \text{mm}^{-1}$, and $\mu_{a2} = 0.024\ \text{mm}^{-1}$. [This wavelength is close to the one used for the time-domain measurements in this study ($\lambda = 528$ nm). Thus no significant differences are expected because of the different wavelengths because the reduced scattering coefficient of polystyrene and the absorption coefficient of graphite are smooth functions of the wavelength in this λ range.] The comparison of these values with those obtained in the time domain revealed that the reduced scattering coefficients are smaller and the absorption coefficients are greater by ~20%–30%. This effect can be explained by delayed scattering. Yaroslavsky *et al.*[36] derived that the product $\mu_a(\mu_a + \mu_s')$ is constant for the optical coefficients obtained with measurements in both the steady-state and the time domains. (For a semi-infinite geometry the condition $\rho \gg z_b, z_0$ must be fulfilled.) Remarkably, this is true for our measurements with errors smaller than 1% for both layers.

References

1. T. J. Farrell, M. S. Patterson, and M. Essenpreis, "Influence of layered tissue architecture on estimates of tissue optical properties obtained from spatially resolved diffuse reflectometry," Appl. Opt. **37,** 1958–1972 (1998).
2. J. T. Bruulsema, J. E. Hayward, T. J. Farrell, M. S. Patterson, L. Heinemann, M. Berger, T. Koschinsky, J. Sandahl-Christiansen, H. Orskov, M. Essenpreis, G. Schmelzeisen-Redeker, and D. Böcker, "Correlation between blood glucose concentration in diabetics and noninvasively measured tissue optical scattering coefficient," Opt. Lett. **22,** 190–192 (1997).
3. B. Change, S. Nioka, J. Kent, K. McCully, M. Fountain, R. Greenfeld, and G. Holtom, "Time-resolved spectroscopy of hemoglobin and myoglobin in resting and ischemic muscle," Anal. Biochem. **174,** 698–707 (1988).
4. E. Gratton, S. Fantini, M. A. Franceschini, G. Gratton, and M. Fabiani, "Measurements of scattering and absorption changes in muscle and brain," Philos. Trans. R. Soc. London Ser. B **352,** 727–735 (1997).
5. E. Okada, M. Firbank, and D. T. Delpy, "The effect of overlying tissue on the spatial sensitivity profile of near-infrared spectroscopy," Phys. Med. Biol. **40,** 2093–2108 (1995).
6. R. A. Weersink, J. E. Hayward, K. R. Diamond, and M. S. Patterson, "Accuracy of noninvasive in vivo measurements of photosensitizer uptake based on a diffusion model of reflectance spectroscopy," Photochem. Photobiol. **66,** 326–335 (1997).
7. M. S. Patterson, B. Chance, and B. C. Wilson, "Time resolved reflectance and transmittance for the noninvasive measurement of tissue optical properties," Appl. Opt. **28,** 2331–2336 (1989).
8. R. C. Haskell, L. O. Svaasand, T. T. Tsay, T. C. Feng, M. McAdams, and B. J. Tromberg, "Boundary conditions for the diffusion equation in radiative transfer," J. Opt. Soc. Am. A **11,** 2727–2741 (1994).
9. A. Kienle and M. S. Patterson, "Improved solutions of the steady-state and time-resolved diffusion equations for reflectance from a semi-infinite turbid medium," J. Opt. Soc. A **14,** 246–254 (1997).

10. A. Ishimaru, *Wave Propagation and Scattering in Random Media* (Academic, New York, 1978), Chaps. 7 and 9.
11. S. Takatani and M. D. Graham, "Theoretical analysis of diffuse reflectance from a two-layer tissue model," IEEE Trans. Biomed. Eng. **BME-26,** 656–664 (1979).
12. J. M. Schmitt, G. X. Zhou, E. C. Walker, and R. T. Wall, "Multilayer model of photon diffusion in skin," J. Opt. Soc. Am. A **7,** 2141–2153 (1990).
13. I. Dayan, S. Havlin, and G. H. Weiss, "Photon migration in a two-layer turbid medium. A diffusion analysis," J. Mod. Opt. **39,** 1567–1582 (1992).
14. R. Nossal, J. Kiefer, G. H. Weiss, R. Bonner, H. Taitelbaum, and S. Havlin, "Photon migration in layered media," Appl. Opt. **27,** 3382–3391 (1988).
15. H. Taitelbaum, S. Havlin, and G. H. Weiss, "Approximate theory of photon migration in a two-layer medium," Appl. Opt. **28,** 2245–2249 (1989).
16. A. H. Hielscher, H. Liu, B. Chance, F. K. Tittel, and S. L. Jacques, "Time-resolved photon emission from layered turbid media," Appl. Opt. **35,** 719–728 (1996).
17. B. Gélébart, E. Tinet, J.-M. Tualle, S. Avrillier, and J. P. Ollivier, "Réflectance résolue dans le temps et dans l'espace appliquée à l'analyse de milieux en couches," J. Opt. **28,** 234–344 (1997).
18. A. Kienle and R. Hibst, "New optical wavelength for treatment of portwine stains?," Phys. Med. Biol. **40,** 1559–1576 (1995).
19. A. Kienle, M. S. Patterson, N. Utke, R. Bays, G. Wagnières, and H. van den Bergh, "Noninvasive determination of the optical properties of two-layered turbid media," Appl. Opt. **37,** 779–791 (1998).
20. M. Bassani, F. Martelli, G. Zaccanti, and D. Contini, "Independence of the diffusion coefficient from absorption: experimental and numerical evidence," Opt. Lett. **22,** 853–855 (1997).
21. T. Durduran, A. G. Yodh, B. Chance, and D. A. Boas, "Does the photon-diffusion coefficient depend on absorption?," J. Opt. Soc. Am. A **14,** 3358–3365 (1997).
22. T. Nakai, G. Nishimura, K. Yamamoto, and M. Tamura, "Expression of optical diffusion coefficient in high-absorption turbid media," Phys. Med. Biol. **42,** 2541–2549 (1997).
23. B. C. Wilson and G. Adam, "A Monte Carlo model for the absorption and flux distribution of light in tissue," Med. Phys. **10,** 824–830 (1983).
24. L. G. Henyey and J. L. Greenstein, "Diffuse radiation in galaxy," Astrophys. J. **93,** 70–83 (1941).
25. R. Graaff, M. H. Koelink, F. F. M. de Mul, W. G. Zijlstr, A. C. M. Dassel, and J. G. Aarnoudse, "Condensed Monte Carlo simulations for the description of light transport," Appl. Opt. **32,** 426–434 (1993).
26. A. Kienle and M. S. Patterson, "Determination of the optical properties of turbid media from a single Monte Carlo simulation," Phys. Med. Biol. **41,** 2221–2227 (1996).
27. P. R. Bevington, *Data Reduction and Error Analysis for the Physical Sciences* (McGraw-Hill, New York, 1983), Chap. 11.
28. T. Glanzmann, J.-P. Ballini, P. Jichlinski, P. Grosjean, H. van den Bergh, and G. Wagnières, "Tissue characterization by time-resolved fluorescence spectroscopy of endogenous and exogenous fluorochromes: apparatus design and preliminary in vivo and ex vivo results," in *Optical Biopsies and Microscopic Techniques*, I. Bigio, ed., Proc. SPIE **2926,** 41–50 (1996).
29. R. Bays, G. Wagnières, D. Robert, J.-F. Theumann, A. Vitkin, J.-F. Savary, P. Monnier, and H. van den Bergh, "Three-dimensional optical phantom and its application in photodynamic therapy," Laser Surg. Med. **21,** 227–234 (1997).
30. G. C. Beck, N. Akgün, A. Rück, and R. Steiner, "Design and characterization of a tissue phantom system for optical diagnostics," Las. Med. Sci. (in press).
31. G. Alexandrakis, T. J. Farrell, and M. S. Patterson, "Accuracy of the diffusion approximation in determining the optical properties of a two-layer turbid medium," in *Advances in Optical Imaging and Photon Migration*, J. G. Fujimoto and M. S. Patterson, eds., Vol. 21 of OSA Trends in Optics and Photonics Series (Optical Society of America, Washington, D.C., 1998), pp. 11–14.
32. J. B. Fishkin, O. Coquoz, E. R. Anderson, M. Brenner, and B. J. Tromberg, "Frequency-domain photon migration measurements of normal and malignant tissue optical properties in a human subject," Appl. Opt. **36,** 10–20 (1997).
33. A. Kienle and M. S. Patterson, "Determination of the optical properties of semi-infinite turbid media from frequency-domain reflectance close to source," Phys. Med. Biol. **42,** 1801–1819 (1997).
34. D. T. Delpy, M. Cope, P. van der Zee, S. R. Arridge, S. Wray, and J. S. Wyatt, "Estimation of optical pathlength through tissue from direct time of flight measurement," Phys. Med. Biol. **33,** 1433–1442 (1988).
35. J. M. Tualle, B. Gélébart, E. Tinet, S. Avrillier, and J. P. Ollivier, "Real time optical coefficients evaluation from time and space resolved reflectance measurements," Opt. Commun. **124,** 216–221 (1996).
36. I. V. Yaroslavsky, A. N. Yaroslavsky, V. V. Tuchin, and H.-J. Schwarzmaier, "Effect of the scattering delay on time-dependent photon migration in turbid media," Appl. Opt. **36,** 6529–6538 (1997).